Resonant two-photon ionization spectroscopy of jet-cooled PdC

Jon D. Langenberg, Lian Shao, and Michael D. Morse[a)]
Department of Chemistry, University of Utah, Salt Lake City, Utah 84112

The first optical investigation of the spectra of diatomic PdC has revealed that the ground state has $\Omega = 0^+$, with a bond length of $r_0 = 1.712$ Å. The Hund's case (a) nature of this state could not be unambiguously determined from the experimental data, but dispersed fluorescence studies to be reported in a separate publication, in combination with a comparison to theoretical calculations, demonstrate that it is the $2\delta^4 12\sigma^2$, $^1\Sigma_{0^+}^+$ state, which undergoes spin–orbit mixing with a low-lying $2\delta^4 12\sigma^1 6\pi^1$, $^3\Pi_{0^+}$ state. An excited $^3\Sigma^+$ state with $r_e = 1.754 \pm 0.003$ Å ($r_0 = 1.758 \pm 0.002$ Å) and $\Delta G_{1/2} = 794$ cm^{-1} is found at $T_0 = 17\,867$ cm^{-1}. Although only the $\Omega = 1$ component of this state is directly observed, the large hyperfine splitting of this state for the ^{105}Pd ^{12}C isotopomer implies that an unpaired electron occupies an orbital that is primarily of $5s$ character on Pd. Comparison to *ab initio* calculations identifies this state as $2\delta^4 12\sigma^1 13\sigma^1$, $^3\Sigma_1^+$. To higher wavenumbers a number of transitions to states with $\Omega = 0^+$ have been observed and rotationally analyzed. Two groups of these have been organized into band systems, despite the clear presence of homogeneous perturbations between states with $\Omega = 0^+$ in the region between 22 000 and 26 000 cm^{-1}. © *1999 American Institute of Physics.* [S0021-9606(99)00531-0]

I. INTRODUCTION

Owing to the importance of transition metal based catalysts for the controlled reduction, oxidation, and reforming of carbon based molecules, there has recently been much interest in the diatomic transition metal carbides. These molecules provide the smallest units in which the transition metal–carbon bond is present, and it is reasonable to think that knowledge gained by investigations of these diatomic molecules will be at least partially transferable to larger systems. Within the past five years optical spectroscopic studies of FeC,[1,2] CoC,[3,4] YC,[5] NbC,[6] IrC,[7] and PtC (Refs. 8, 9) have been published. In addition, VC,[10,11] NbC,[11] and RhC,[12] have been studied by electron spin resonance spectroscopy in cryogenic rare gas matrices over an extended period of time. Recently laser spectroscopic studies of FeC,[13] MoC,[14] and RuC (Ref. 15) have been published from this research group, and a paper on the optical spectra of NiC is in preparation.[16] In an earlier period of interest in the carbides RuC,[17,18] RhC,[19–21] PtC,[22–25] and IrC[26,27] were investigated by conventional optical methods in high temperature King furnaces. In this paper we report spectra of PdC, which is studied to add to the growing body of knowledge surrounding the transition metal carbides.

In addition to these experimental studies of the diatomic transition metal carbides, a growing number of theoretical studies have been published as well. These include older investigations of TiC,[28] CrC,[29] YC,[30] and RuC (Ref. 31) along with more recent studies of TiC,[32] VC,[33] CrC,[34] RhC,[35] IrC,[36] and TaC.[37] Diatomic PdC has itself been studied theoretically on five occasions. Shim and Gingerich used all-electron Hartree–Fock/configuration interaction (HF/CI) calculations,[38,39] Pacchioni *et al.* used a pseudopotential mul-

tireference double-excitation configuration interaction (PP–MRD–CI) method,[40] and Russo *et al.* used a local spin density formalism.[41] In recent work Tan *et al.* have investigated the molecule using a complete active space multiconfiguration self-consistent field (CAS–MCSCF) method followed by first-order configuration interaction (FOCI) and multireference singles+doubles configuration interaction (MRSDCI).[42] Most recently, Shim and Gingerich have reinvestigated the PdC molecule using a multireference configuration interaction method which treats relativistic effects using perturbation theory.[43] Despite the number of these studies, even the identity of the ground electronic state of PdC remains in dispute.

The early HF/CI studies by Shim and Gingerich predicted a $^3\Sigma^-$ ground state arising from the $11\sigma^2 2\delta^4 6\pi^2$ configuration,[38,39] as did the PP–MRD–CI study of Pacchioni *et al.*;[40] the local spin density study obtained a $^1\Sigma^+$ ground state arising from the $11\sigma^2 2\delta^4 12\sigma^2$ configuration;[41] and the CAS–MCSCF–MRSDCI study of Tan *et al.* predicted a near-degeneracy between the $^1\Sigma^+$ state arising from the $11\sigma^2 2\delta^4 12\sigma^2$ configuration and the $^3\Pi$ state arising from the $11\sigma^2 2\delta^4 12\sigma^1 6\pi^1$ configuration.[42] The most recent work of Shim and Gingerich identifies the ground state as the $11\sigma^2 2\delta^4 12\sigma^2$, $^1\Sigma^+$ state,[43] in agreement with Russo *et al.*[41] By providing the first spectroscopic study of the PdC molecule, it was our hope to resolve these issues and to establish the nature of the ground state of the molecule.

II. EXPERIMENT

In the present study, diatomic PdC was examined by resonant two-photon ionization (R2PI) spectroscopy performed on supersonically cooled molecular beams with time-of-flight mass spectrometric detection. The R2PI instrument consisted of two vacuum chambers, one housing the molecu-

a)Electronic mail: morse@chemistry.chem.utah.edu

lar beam source, and the other the time-of-flight mass spectrometer. Inside the source chamber, PdC molecules were produced by focusing the 532 nm radiation from a pulsed Nd:YAG laser to a 0.5 mm spot on a palladium disk. To remove metal uniformly and to avoid drilling a hole through the sample, the disk was rotated and translated by a system of gears, a cam, and a cam follower.[44] The ablation pulse was timed to coincide with a pulse of helium carrier gas, seeded with approximately 3% methane based on partial pressures. The carrier gas, along with the entrained atoms and molecules, expanded into the source chamber, which was held to approximately 2×10^{-4} Torr by a 10″ diffusion pump. The resulting molecular beam, roughly collimated by a 5 mm conical skimmer, passed into the time-of-flight mass spectrometer, where it was probed by tunable radiation from a Nd:YAG-pumped dye laser. Molecules absorbing this radiation were then ionized by 193 nm radiation from an excimer laser operating on an ArF mixture. The resulting ions were separated by mass and detected with a microchannel plate detector. The output from the detector was then amplified, digitized, and stored in a computer for later analysis. This entire experimental cycle was repeated at a rate of 10 Hz.

The spectrum of PdC was initially scanned with the dye laser in low resolution (0.7 cm^{-1}) to survey the vibronic bands. To measure the lifetimes of the upper states of these bands the dye laser was tuned to the individual transitions, and the PdC^{+} signal intensity was monitored while the computer scanned the delay between the firing of the excitation laser and the ionization laser. The resulting curve was fit to an exponential decay using a nonlinear least squares algorithm,[45] and the $1/e$ lifetime was thereby extracted. The results of three or more separate measurements were averaged to obtain a final value.

To investigate the fine structure of the bands, an air-spaced *étalon* was placed in the cavity of the dye laser to narrow the linewidth (0.04 cm^{-1}), and the cavity was pressure scanned with Freon-12. The high resolution scans were calibrated using either the I$_2$ absorption atlas[46] (corrected for the error),[47] the heated I$_2$ atlas,[48] or the Te$_2$ atlas.[49] Because the probe laser was propagated against the flow of the molecular beam, the spectra were also corrected for the Doppler shift experienced by the PdC molecules as they traveled toward the radiation source at the beam velocity of helium (1.77×10^5 cm·s^{-1}), a correction which never amounted to more than 0.16 cm^{-1}. For absolute calibration of the bands above 23 800 cm^{-1} the output of a near infrared dye laser was frequency doubled and the fundamental radiation was used for calibration while the second harmonic was used for excitation. The second harmonic generation was accomplished with a KDP crystal which was angle-tuned to the optimum position for the wavelength of interest, and the dye laser was then pressure scanned. The crystal did not detune significantly over the pressure scan range, which was typically 10 cm^{-1}.

III. RESULTS

As displayed in the mass spectrum of Fig. 1, laser ablation of metallic palladium in the presence of the methane-
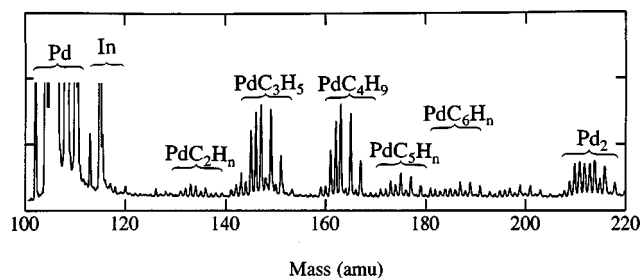

FIG. 1. Mass spectrum obtained by laser ablation of a palladium sample in a pulsed supersonic jet of 3%CH$_4$ in helium, using ArF excimer radiation (6.42 eV, 193 nm) for photoionization. In addition to atomic palladium, a small amount of indium impurity is efficiently detected because it is one-photon ionized at 193 nm. A number of palladium hydrocarbons are identified in the mass spectrum, with particularly clean signals arising for PdC$_3$H$_5$ and PdC$_4$H$_9$. These display the characteristic pattern of Pd isotopic abundances, clearly establishing that the remainder of the molecule has a mass of 41 and 57, respectively.

seeded carrier gas produced a number of identifiable Pd-hydrocarbon species, including PdC$_2$H$_n$, PdC$_3$H$_5$, PdC$_4$H$_9$, PdC$_5$H$_n$, and PdC$_6$H$_n$, as well as Pd$_2$. Ion signals for each of these species were collected; however, no transitions were found for any of the palladium hydrocarbon compounds. Because the mass spectrum shown in Fig. 1 was collected under high ionization laser fluence, it is possible that the palladium hydrocarbons observed result from multiphoton ionization/fragmentation processes of larger species. This would account for the lack of observable spectra. A series of transitions between 14 600 cm^{-1} and 17 800 cm^{-1} were observed in the masses corresponding to the various isotopes of Pd$_2$. These will be investigated further and reported in a future publication.

PdC produced no off-resonance signal in the mass spectrum; however, there was interference from an abnormally high background. The background mass spectrum was broad and ill-defined, unlike the usually sharp mass spectrum peaks. The likely cause of this broad, featureless background was multiphoton ionization and fragmentation of diffusion pump oil. The problem was solved by placing a copper box, in thermal contact with a Dewar at liquid nitrogen temperature, around the ionization region. This arrangement removed the diffusion pump oil from the ionization region and greatly diminished the background at the mass of PdC^{+}.

The spectrum of PdC was scanned under low resolution conditions from 14 145 cm^{-1} to 27 200 cm^{-1}, and consisted of approximately 50 bands. The lowest energy band appeared near 17 867 cm^{-1}, one of three between 17 800 cm^{-1} and 19 800 cm^{-1}. The next band did not appear until 21 800 cm^{-1}. A portion of the low resolution spectrum between 21 600 cm^{-1} and 25 400 cm^{-1} is displayed in Fig. 2. Twenty-nine of the bands were rotationally resolved and analyzed; most of these were satisfactorily fit to the simple expression

$$\nu_0 = B'J'(J'+1) - B''J''(J''+1). \tag{3.1}$$

Identification of the J values of the first lines allowed the Ω quantum numbers to be determined without ambiguity. A
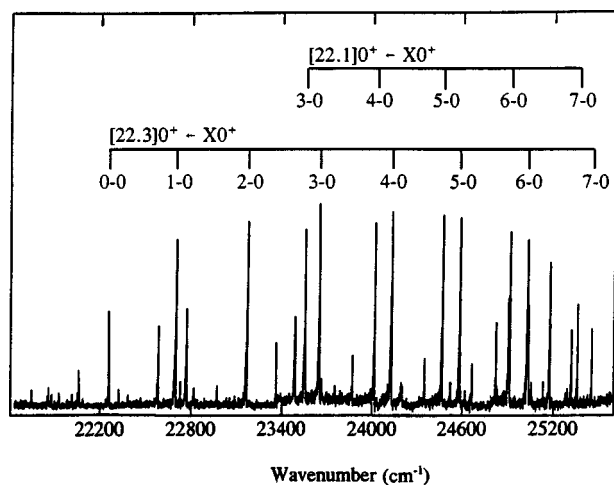
FIG. 2. Vibronically resolved spectrum of ^{108}Pd ^{12}C, over the range 21 600–25 600 cm^{-1}. Vibrational progressions of the $[22.1]0^+\leftarrow X0^+$ and $[22.3]0^+\leftarrow X0^+$ band systems are indicated.

summary of these rotational fits is given in Table I, which also provides isotope shifts and excited state lifetimes for the observed bands.

Based on the lower state rotational constants and Ω'' values, it appears that all of the transitions arise from the same lower state, which is presumably the ground state of the molecule. Accordingly, the rotational constant of the lower state was required to be the same for all of the unperturbed bands, which were fit simultaneously to extract the most accurate values of B_0'' for the various isotopomers. This ground vibronic state has $\Omega''=0$. Three band systems were identified in the spectrum and are discussed below. Their spectroscopic constants are collected in Table II, which displays all of the electronic states of PdC which have been characterized in this work. In addition, a number of bands were observed which could not be classified into band systems. Data pertinent to these unclassified, but rotationally analyzed bands are provided in Table I.

TABLE I. Rotationally resolved bands of ^{108}Pd ^{2}C.[a]

Band System	$v'-v''$	v_0 (cm^{-1})	Isotope Shift (cm^{-1})[b]	B_v' (cm^{-1})	λ_v' (cm^{-1})	r_v' (Å)	τ (μs)
$[17.9]^3\Sigma^+\leftarrow X0^+$	0–0	17 867.0328(623)	−0.006(91)	0.504 91(120)	8.262(676)	1.758 3(21)	0.503(31)
	1–0	18 660.7493(704)	−1.103(104)	0.499 88(167)	8.215(1.207)	1.767 1(30)	0.514(7)
$[22.3]0^+\leftarrow X0^+$	0–0	22 253.5301(25)	0.1327(35)	0.430 009(36)	Not applicable	1.905 32(8)	0.386(2)
	1–0	22 685.4603(32)	−0.7819(51)	0.429 150(69)	Not applicable	1.907 22(15)	0.274(5)
	2–0	23 152.1891(30)	−1.1362(40)	0.426 149(90)	Not applicable	1.913 92(20)	0.245(3)
	3–0	23 638.7036(15)	−1.7477(20)	0.421 119(44)	Not applicable	1.925 32(10)	0.264(2)
	4–0	24 118.7258(33)	−2.2783(45)	0.414 576(64)	Not applicable	1.940 46(15)	0.241(7)
	5–0	24 577.7072(64)	−2.3476(86)	0.397 963(39)	Not applicable	1.980 54(10)	0.240(1)
	6–0				Not applicable		0.093(3)
	7–0	25 445.7514(25)	−3.2477(41)	0.383 632(78)	Not applicable	2.017 20(21)	0.274(2)
$[22.1]0^+\leftarrow X0^+$	3–0	23 546.0557(20)	−1.7811(28)	0.389 277(54)	Not applicable	2.002 52(14)	2.75(5)
	4–0	24 006.2499(25)	−2.4253(34)	0.385 745(57)	Not applicable	2.011 66(15)	1.42(1)
	5–0	24 459.0106(42)	−3.0074(47)	0.381 075(59)	Not applicable	2.023 95(16)	1.14(2)
	6–0	24 904.9719(391)[c]		0.377 002(1311)[c]	Not applicable	2.034 9(35)	1.00(6)
	7–0	25 348.7296(32)	−4.0025(45)	0.373 671(39)	Not applicable	2.043 91(11)	1.50(5)
	8–0	25 772.6473(332)[c]		0.367 512(777)[c]	Not applicable	2.060 96(218)	0.397(7)
Unclassified Bands		22 053.2064(30)	0.0147(56)	0.413 762(170)	Not applicable	1.942 36(40)	1.06(1)
		22 569.3035(24)	−0.3927(39)	0.404 444(115)	Not applicable	1.964 61(28)	2.02(6)
		22 752.5546(26)	−4.8795(36)	0.483 557(54)	Not applicable	1.796 73(10)	0.459(13)
		23 351.7513(141)	0.0068(259)[d]	0.430 707(361)	Not applicable	1.903 77(80)	0.419(10)
		23 474.8261(20)	−5.9551(32)	0.480 675(98)	Not applicable	1.802 10(18)	0.475(3)
		23 860.3288(114)	−0.7304(125)	0.413 111(396)	Not applicable	1.943 89(93)	0.514(1)
		24 658.4429(42)	−0.3119(62)	0.373 926(37)	Not applicable	2.043 21(10)	1.44(4)
		24 897.298(39)[c]	Not analyzed	0.464 64(131)[c]	Not applicable	1.832 94(258)[c]	
		24 813.6402(67)	−2.2734(91)	0.396 703(72)	Not applicable	1.983 69(18)	0.573(21)
		25 165.2538(18)	−1.3127(42)	0.374 497(68)	Not applicable	2.041 65(19)	0.870(13)
		25 309.5009(31)	−2.5483(55)	0.381 893(46)	Not applicable	2.021 78(12)	0.864(39)
		25 652.4323(56)	−2.5339(88)	0.375 205(99)	Not applicable	2.039 72(27)	0.4(1)
		25 758.353(35)[c]	Not analyzed	0.443 63(98)[c]	Not applicable	1.875 84(207)[c]	

[a]Fitted values of B_0'' are: 0.534 742(76) for ^{104}Pd ^{12}C; 0.534 016(54) for ^{105}Pd ^{12}C; 0.533 556(60) for ^{106}Pd ^{12}C; 0.532 470(55) for ^{108}Pd ^{12}C; and 0.531 645(68) for ^{110}Pd ^{12}C. These were obtained from a simultaneous fit of all of the unperturbed bands and convert to r_0'' values of: 1.711 86(12), 1.712 18(9), 1.712 00(10), 1.712 21(9), and 1.711 98(11), respectively. In this and all other cases, quoted error limits represent 1σ in the least-squares fit of the data.
[b]Isotope shift is defined as $v_0(^{108}$Pd ^{12}C$) - v_0(^{105}$Pd ^{12}C$)$.
[c]Determined from a deperturbation analysis as described in the text. For the 24 900 cm^{-1} pair of levels, H_{12} is determined to be 2.8848(313) cm^{-1} from the least-squares fit. For the 25 765 cm^{-1} pair, H_{12} is determined to be 2.7971(524) cm^{-1}.
[d]Isotope shift estimated from the value of $v_0(^{108}$Pd ^{12}C$) - v_0(^{106}$Pd ^{12}C$)$.

TABLE II. Electronic states of ^{108}Pd ^{12}C.[a]

Electronic State[b]	T_0 (cm^{-1})	ω_e (cm^{-1})	$\omega_e x_e$ (cm^{-1})	$\omega_e y_e$ (cm^{-1})	B_e (cm^{-1})	α_e (cm^{-1})	r_e (Å)	τ (μs)	h (cm^{-1})
[22.3]0$^+$	22 251.06(6.12)[c]	400.89(11.67)[c]	$-22.225(3.449)$[c]	$-2.03(28)$[c]	0.440 17(436)[c]	0.007 00(201)[c]	1.8832(93)[c]	~0.256	
[22.1]0$^+$	22 131.86(4.22)[d]	483.37(1.96)[d]	2.98(0.18)[d]		0.403 15(75)[d]	0.003 94(32)[d]	1.967 76(182)[d]	~1.35	
[17.9]$^3\Sigma^+$	17 867.0328(623)	$\Delta G_{1/2}$=793.716(94)			0.507 42(198)[e]	0.005 0(21)	1.7540(34)	0.508	±0.030(5)
X0$^+$	0.00				B_0=0.532 470(55)		r_0=1.712 21(9)		

[a]Values given in parentheses represent the 1σ error limit of the fitted parameter, in units of the last digit quoted.

[b]The electronic state is identified by the location of its $v=0$ level, measured in units of 1000 cm^{-1}, in square brackets.

[c]Both the vibrational fit to extract T_0, ω_e, and $\omega_e x_e$, and the rotational fit to extract B_e and α_e for the [22.3]0$^+$ state were unsatisfying because of the large residuals obtained in the fit. Even with the inclusion of an $\omega_e y_e$ term, the residuals in the vibrational fit were as large as 6.6 cm^{-1}. Omitting this term, the residuals increased to 23 cm^{-1}. Likewise, the residuals on the fit of B_e and α_e were as large as 0.0066 cm^{-1}. These facts indicate extensive perturbations in the [22.3]0$^+$ state, and explain the large error limits obtained for the spectroscopic parameters.

[d]The fit of the vibrational levels of the [22.1]0$^+$ state omitted the $v'=6$, 8 levels, since the deperturbation procedure introduced greater errors in the $T_{v'}$ values than for the remaining levels. The energies of the $v'=6$ and 8 levels calculated from the vibrational constants listed above are 24 904.97 and 25 772.65 cm^{-1}, respectively, however. These are 2.02 and 11.74 cm^{-1} above the deperturbed energies, respectively, suggesting that perturbations by another state may also be important. Likewise, the $v'=6$ and $v'=8$ levels were omitted from the fit of the B_v' values to extract B_e' and α_e'. The values of B_6' and B_8' predicted from the fit are 0.377 563 and 0.369 674 cm^{-1}, respectively. These are 0.000 56 and 0.002 16 cm^{-1} larger than the corresponding deperturbed values, which are listed in Table I.

[e]The fitted λ_v values of the $v=0$ and $v=1$ levels of the [17.9]$^3\Sigma^+$ state of ^{108}Pd ^{12}C are 8.262±0.676 and 8.215±1.207 cm^{-1}, respectively.

A. The [17.9] $^3\Sigma_1^+\leftarrow X0^+$ band system

The [17.9]1$\leftarrow$X0 system consists of two members: the 0–0 band, near 17 867 cm^{-1}, and the 1–0 band, near 18 661 cm^{-1} for ^{108}Pd ^{12}C. As is evident in the rotationally resolved scan of the 0–0 band displayed in Fig. 3, no band head appears in the spectrum. However, the R-lines become more closely spaced toward higher J, while the P-lines become more widely spaced at higher J, indicating that an R-head is expected to form at higher values of J than are populated in our experiment. In contrast, the Q-lines fan out to the blue, and therefore cannot be fit with the same value of B'. This implies that there is Λ-doubling in the upper state. To account for the Λ-doubling, the rotational model of Eq. (3.1) was revised according to[50]

$$\nu_{P,R/Q}=\nu_0+(B'\pm q'/2)J'(J'+1)-B''J''(J''+1),$$
(3.2)

where the upper sign is associated with e levels of the upper state, the lower sign with f levels. As justified below, it was assumed that the lower state is an $\Omega''=0^+$ state, which pos-
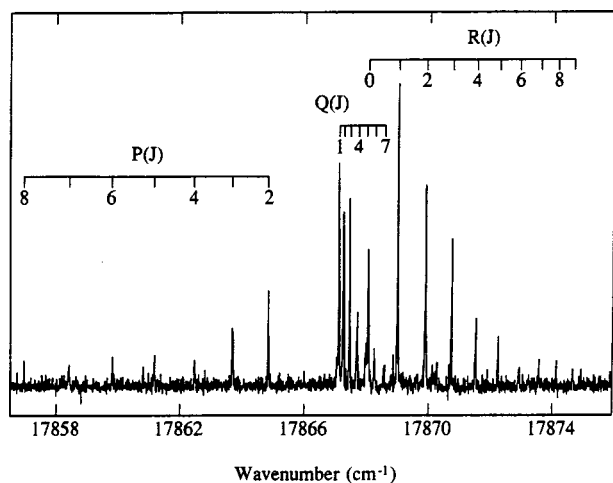
sesses only e levels. As such, the upper sign was used for the P- and R-branches, which obey the selection rule $e\leftrightarrow e$, $f\leftrightarrow f$.[51] The lower sign was used for the Q-branch, which obeys the selection rule $e\leftrightarrow f$, $f\leftrightarrow e$.[51] Formula (3.2) is the accepted form for a $^1\Pi_2$ upper state,[50] but similar expressions are valid for any $\Omega=1$ state if the perturber that is responsible for the Λ-doubling is remote in energy.

Attempts to fit the line positions using Eq. (3.2) met with limited success. The residuals in the fit are significantly larger than the laser linewidth used to record the spectrum, and display a systematic trend, clearly showing that Eq. (3.2) is inadequate to describe the observed Λ-doubling. This indicates that the perturber is not energetically remote, so that the perturbation theory expression for the Λ-doubling in Eq. (3.2) is invalid. Recent theoretical investigations,[42,43] discussed more fully below, suggest that the [17.9]1 state is the $\Omega=1$ component of a $^3\Sigma^+$ state deriving from the $2\delta^4 12\sigma^1 13\sigma^1$ configuration. For such an upper state the $\Omega=0^-$ component is invisible from an $\Omega=0^+$ lower state, unless it is strongly mixed with the f levels of the $\Omega=1$ component, as occurs when the $^3\Sigma^+$ state approaches Hund's case (b). On the basis of the theoretical calculations, an attempt was made to fit the rotational lines using the expressions for the $\Omega=1$ levels of a $^3\Sigma^+$ state which result from a diagonalization of its matrix Hamiltonian,[52] according to

$$\nu_{P,R}(J'')=\nu_0+B'J'(J'+1)-B''J''(J''+1),$$
(3.3a)

and

$$\nu_Q(J'')=\nu_0+B'J'(J'+1)+B'-\lambda'+[(B'-\lambda')^2$$
$$+4(B'-\gamma'/2)^2J'(J'+1)]^{1/2}-B''J''(J''+1).$$
(3.3b)

FIG. 3. Rotationally resolved scan over the 0–0 band of the [17.9]$^3\Sigma_1^+$ $\leftarrow X0^+$ system of ^{108}Pd ^{12}C.

For this fit the rotational constant of the ground state, B'', was held fixed at the value determined from a simultaneous fit of the unperturbed bands, and γ' was set to zero because the limited number of rotational levels observed did not permit it to be accurately determined.

The least-squares fits of the rotational lines to the model of Eq. (3.3) provided consistent values of B' and λ' for the $v=0$ and $v=1$ levels for all isotopic modifications, and reduced the magnitude of the residuals to values comparable to the unperturbed bands. This provides convincing evidence that the [17.9]1 state is the $\Omega=1$ component of a $^3\Sigma$ state. In addition, the fact that it is the Q-branch, rather than the R- and P-branches, that follows the complicated formula given in Eq. (3.3b) demonstrates that the levels reached in the Q-branch have the same e/f parity as the unobserved $\Omega=0$ level of the [17.9]$^3\Sigma$ state. Since the Q-branch obeys the selection rule $e\leftrightarrow f$, $f\leftrightarrow e$,[51] this establishes that the $\Omega=0$ ground state and the $\Omega=0$ component of the [17.9]$^3\Sigma$ state have opposite e/f parity. Assuming that the ground state is of 0^+ parity, as justified below, this establishes the upper state as $^3\Sigma^+$, in agreement with *ab initio* calculations.

Spectroscopic constants derived for this system and all other rotationally resolved bands are given in Table I for ^{108}Pd ^{12}C. The measured rotational line positions for the various isotopomers of PdC for this and all other rotationally analyzed bands are available from the author (M.D.M.) or the Physics Auxiliary Publication Service (PAPS).[53]

Additional support for the assignment of the upper state to a $^3\Sigma^+$ state deriving from the $2\delta^4 12\sigma^1 13\sigma^1$ configuration is found in the hyperfine splitting observed in the ^{105}Pd ^{12}C isotope. The ^{105}Pd nucleus is magnetic ($I=5/2$), and the lines of the [17.9]1$\leftarrow$X0 system of the ^{105}Pd ^{12}C isotopomer were split by hyperfine interactions. For the low-J rotational levels of this state, prior to the transition to Hund's case (b), this is expected to follow the formulas developed by Frosch and Foley for the a_β coupling case,[54] in which the electronic angular momenta $\hat{\mathbf{L}}$ and $\hat{\mathbf{S}}$ have well-defined projections on the molecular axis, Λ and Σ, respectively, and the total angular momentum apart from nuclear spin, J, defines the rotational energy levels. Coupling of $\hat{\mathbf{J}}$ with the nuclear spin, $\hat{\mathbf{I}}$, then leads to the total angular momentum, $\hat{\mathbf{F}}$, with the hyperfine contribution to the energy given to first order in perturbation theory by[54]

$$E_{hf}(S,\Lambda,\Sigma,\Omega,I,J,F)=h\Omega\left[\frac{F(F+1)-I(I+1)-J(J+1)}{2J(J+1)}\right].$$
(3.4)

In this formula

$$h=a\Lambda+\left(b_F+\frac{2}{3}c\right)\Sigma,$$
(3.5)

where

$$a=2.000g_I\beta_e\beta_n\langle r^{-3}\rangle,$$
(3.6)

$$b_F=g_eg_I\beta_e\beta_n\frac{8\pi}{3}|\psi(0)|^2,$$
(3.7)

and

$$c=\tfrac{3}{2}g_eg_I\beta_e\beta_n\langle 3\cos^2\theta-1\rangle\langle r^{-3}\rangle.$$
(3.8)

Here $g_e=2.0023193$ is the electronic g-factor,[55] $g_I\equiv\mu_I/I$ is the nuclear g-factor, given by the nuclear magnetic dipole moment in nuclear magnetons divided by the nuclear spin, I; β_e is the Bohr magneton; β_n is the nuclear magneton; θ is
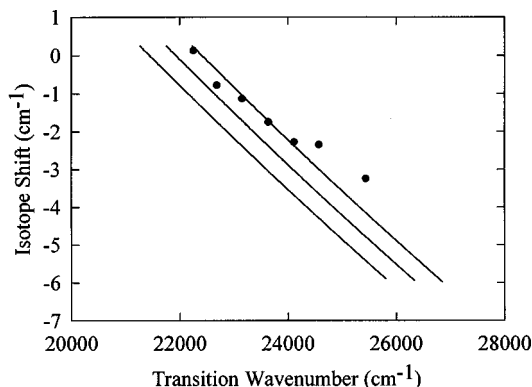

FIG. 4. Measured isotope shifts, $\nu_0(^{108}$Pd ^{12}C$)-\nu_0(^{105}$Pd ^{12}C$)$, of the [22.3]$0^+\leftarrow X0^+$ system (filled circles) along with calculated isotope shifts (solid lines) for assignments in which the 22 253 cm^{-1} band is identified as the 0–0, 1–0, and 2–0 band, in descending order on the graph. From the plot it is clear that the 0–0 assignment is correct.

the angle between the internuclear axis and the vector from the magnetic nucleus to the electron; the expectation values provide averages for the unpaired electron; and $|\psi(0)|^2$ provides the probability density for finding the electron at the magnetic nucleus. The numerical factors $g_e\beta_e\beta_n$ combine to give the value 0.003 186 cm$^{-1}\cdot$bohr^3.[55]

To estimate the hyperfine parameter, h', the spectrum of ^{105}Pd ^{12}C was simulated. Using the fitted spectroscopic constants, and the temperature and laser line width estimated from the simultaneously recorded ^{108}Pd ^{12}C spectrum, the hyperfine parameter h' was varied until the simulation matched the spectrum. This procedure produced a hyperfine parameter of $|h'|=0.030\pm0.005$ cm^{-1} for the [17.9]1 state. The linewidth of the laser employed for this study (0.04 cm^{-1}), combined with other experimental problems, prohibited the determination of the sign of h'. Nevertheless, the magnitude of h' can only be explained by a Fermi contact interaction due to an unpaired electron in an orbital which is primarily $5s_{\text{Pd}}$ in character. This is entirely consistent with the assignment of the [17.9]1 state as the $2\delta^4 12\sigma^1 13\sigma^1,^3\Sigma_1^+$ state.

B. The [22.3]$0^+\leftarrow X0^+$ band system

This band system was the most intense of the three band systems identified, and consisted of nine members, eight of which were rotationally resolved. A list of the rotationally resolved bands of the system, along with fitted spectroscopic constants, is provided in Table I. A plot of measured isotope shifts $[\nu(^{108}$Pd ^{12}C$)-\nu(^{105}$Pd ^{12}C$)]$ as a function of band origin is given in Fig. 4 for the bands which appeared relatively unperturbed, along with calculated isotope shifts based on vibrational numberings in which the band at 22 253 cm^{-1} is assigned as the 0–0, 1–0, or 2–0 band. These calculated isotope shifts were plotted as solid lines by calculating the transition wavenumber as a function of v' using

$$\nu=\nu_0+v'\omega_e'-(v'^2+v')\omega_e'x_e'$$
(3.9)

and the isotope shift as a function of v' as

$$\nu-\nu_i=(1-\rho)[\omega_e'(v'+1/2)-\omega_e''(1/2)]-(1-\rho^2)$$

$$\times[\omega_e'x_e'(v'+1/2)^2-\omega_e''x_e''(1/2)^2],$$
(3.10)
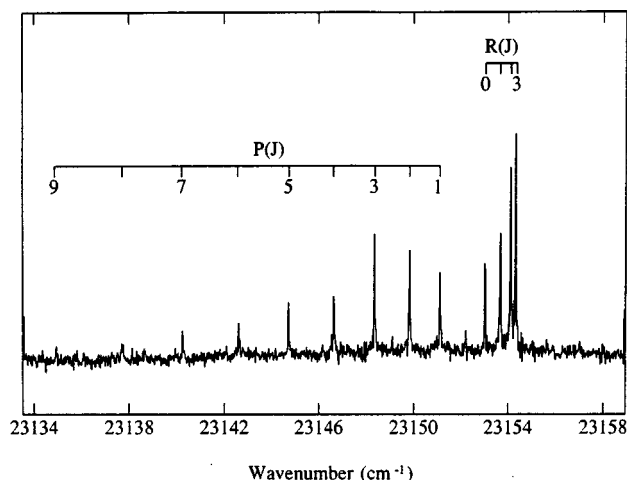
FIG. 5. Rotationally resolved scan over the 2–0 band of the $[22.3]0^+$ $\leftarrow X0^+$ system of PdC.

FIG. 6. Measured isotope shifts, $\nu_0(^{108}\mathrm{Pd}\,^{12}\mathrm{C}) - \nu_0(^{105}\mathrm{Pd}\,^{12}\mathrm{C})$, of the $[22.1]0^+ \leftarrow X0^+$ system (filled circles) along with calculated isotope shifts (solid lines) for assignments in which the 23 546 cm^{-1} band is identified as the 2–0, 3–0, or 4–0 band, in descending order on the graph. From the plot it is clear that the 3–0 assignment is correct.

with ρ given as $(\mu/\mu_i)^{1/2}$.[56] By treating ν and $\nu - \nu_i$ as parametric functions of the continuous parameter v', it was straightforward to generate the curves of calculated isotope shift vs. transition wavenumber displayed in Fig. 4. For this purpose, the values of ω_e'' and $\omega_e'' x_e''$ were taken to be 844 and 5.7 cm^{-1}, respectively, as estimated from dispersed fluorescence work on PdC currently in progress.[57]

From a comparison of the calculated isotope shifts to the observed values, it is clear that the 22 253 cm^{-1} band is properly assigned as the 0–0 band. It is also clear that the 1–0, 5–0, and 7–0 bands fall significantly off the predicted line, indicating the existence of perturbations in these upper states. Perturbations were also evident in the fit of the band origins to extract ω_e and $\omega_e x_e$, since inclusion of just these two vibrational parameters led to a fit of the data with residuals as large as 23 cm^{-1}. Likewise, the measured upper state rotational constants did not fit well to the model $B_v = B_e - (v + 1/2)\alpha_e$, giving residuals as large as 0.0066 cm^{-1} in the fitted values of B_v. The anomalously long lifetime of the $v'=0$ level (386 ns) and the anomalously short lifetime of the $v'=6$ level (93 ns) also provide evidence of perturbations in this system. The remaining vibrational levels of this excited state all display lifetimes within the range of 256 ± 18 ns.

A rotationally resolved scan over the 2–0 band of this system, which occurs near 23 152 cm^{-1}, is displayed in Fig. 5 for the $^{108}\mathrm{Pd}\,^{12}\mathrm{C}$ isotopomer. The absence of a Q-branch and the presence of $R(0)$ and $P(1)$ identifies the system as an $\Omega'=0 \leftarrow \Omega''=0$ system. A large increase in bond length evidently occurs upon electronic excitation in this system, leading to band heads near $R(3)$ in the rotationally resolved spectra. The long bond length of PdC in this electronic state is mirrored in the low vibrational frequency which is found. Although ω_e' is poorly determined for this state due to the many perturbations which are present, its estimated value of 401 cm^{-1} is much less than any vibrational frequency previously reported for a transition metal carbide.
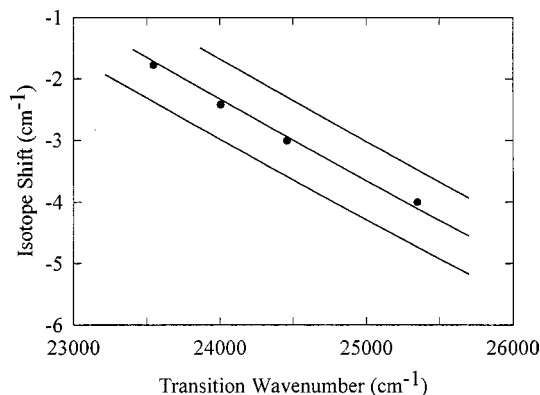
C. The $[22.1]0^+ \leftarrow X0^+$ band system

The $[22.1]0 \leftarrow X0$ band system is nearly as intense as the $[22.3]0 \leftarrow X0$ system. The fine structure of these bands was also bereft of Q-branches and fit to $\Omega'=0 \leftarrow \Omega''=0$ transitions. Six members of the band system were identified; however, in this case the lowest energy band had an isotope shift of $\nu_0(^{108}\mathrm{Pd}\,^{12}\mathrm{C}) - \nu_0(^{105}\mathrm{Pd}\,^{12}\mathrm{C}) = -1.7809(28)$ cm^{-1}, strongly suggesting that it is not an origin band. A plot of the measured isotope shift $[\nu(^{108}\mathrm{Pd}\,^{12}\mathrm{C}) - \nu(^{105}\mathrm{Pd}\,^{12}\mathrm{C})]$ as a function of band position is provided for this system in Fig. 6 for the bands which appeared unperturbed, along with calculated isotope shifts based on vibrational numberings in which the band at 23 546 cm^{-1} is assigned as the 2–0, 3–0, or 4–0 band. From a comparison of the predicted isotope shifts to those observed in the spectrum, it is clear that the 23 546 cm^{-1} band is the 3–0 band.

Perturbations were also clearly evident in the vibrational levels of the $[22.1]0$ state. In particular, the $v'=6$ and $v'=8$ levels were strongly perturbed by other $\Omega=0$ states lying nearby in energy. These perturbing states were also visible in the rotationally resolved spectra, and a sufficient number of rotational lines were observed to perform a two-state deperturbation analysis. After the individual lines had been identified as $R(J)$ or $P(J)$ lines of the higher (or lower) frequency band, total energies were calculated for the upper levels of these transitions by adding the rotational energy of the lower level to the wavenumber of the transition. For this purpose the rotational energy of the lower level was calculated as $B'' J''(J''+1)$, with the value of B'' determined from the simultaneous fit of all unperturbed bands. The resulting energies of the upper and lower members of the perturbing pair of states, designated as $E^+(J)$ and $E^-(J)$, were assumed to be the solutions of a two-state perturbation model in which the Hamiltonian matrix is given as

$$\underline{\underline{H}} = \begin{pmatrix} T^+ + B^+ J(J+1) & H_{12} \\ H_{12} & T^- + B^- J(J+1) \end{pmatrix}. \quad (3.11)$$

The parameters T^+ and B^+ provide the term energy and rotational constant of the higher energy member of the per-
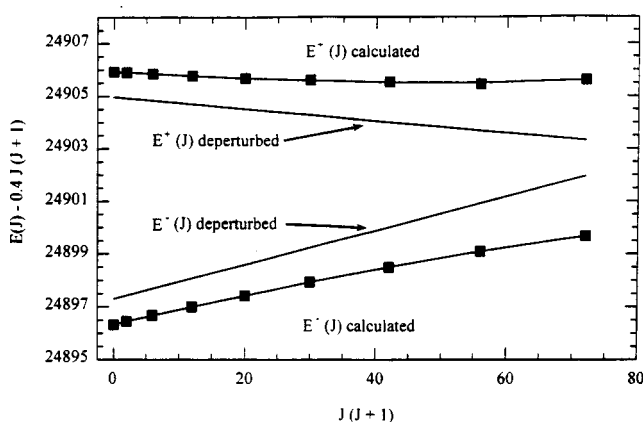
FIG. 7. Deperturbation of the 24 900 cm^{-1} pair of bands. Measured values of $E(J) - 0.4J(J+1)$ for the upper states of the higher and lower frequency bands are displayed as solid squares, along with the fitted curves through these data points, as described in the text and Eq. (3.12). In addition the deperturbed energies, given by $E^{\pm}(J) = T^{\pm} + B^{\pm}J(J+1)$ are given by the straight lines lying between the fitted curves and measured energy levels. In all cases the data are plotted as functions of $J(J+1)$.

turbing pair, while T^- and B^- provide the corresponding parameters for the lower of the two mutually perturbing states. Since both states have the same value of Ω it was assumed that the perturbation matrix element H_{12} is reasonably constant over the small range of J accessed in our experiments. The upper and lower energy levels were simultaneously fit to the eigenvalues of this Hamiltonian matrix, according to

$$E^+(J) = \frac{1}{2}[(T^+ + T^-) + (B^+ + B^-)J(J+1)$$
$$+ \sqrt{[(T^+ - T^-) + (B^+ - B^-)J(J+1)]^2 + 4H_{12}^2}],$$

$$E^-(J) = \frac{1}{2}[(T^+ + T^-) + (B^+ + B^-)J(J+1)$$
$$- \sqrt{[(T^+ - T^-) + (B^+ - B^-)J(J+1)]^2 + 4H_{12}^2}].$$

$$(3.12)$$

In this nonlinear least-squares fit, the parameters T^+, T^-, B^+, B^-, and H_{12} were varied to obtain the best fit.

The resulting fits for the $v' = 6$ and $v' = 8$ levels of ^{108}Pd^{12}C (and for their perturbers) gave root-mean-square values of the residuals of 0.014 and 0.007 cm^{-1}, respectively. These are much smaller than our laser linewidth of 0.04 cm^{-1}, and must be considered excellent fits. The resulting band origins, $T_{v'}$, and rotational constants, $B_{v'}$, are listed in Table I for both the $v' = 6$ and $v' = 8$ levels of the [22.1]0 state and for their perturber levels. Figure 7 presents the measured energy levels $E^+(J), E^-(J)$, and the fitted curve as given in Eq. (3.12), as functions of $J(J+1)$, for the interacting states near 24 900 cm^{-1}. The higher energy member of this pair of perturbing states is the $v' = 6$ level of the [22.1]0 state. In addition, lines describing the behavior of the deperturbed system, governed by the equations

$$E^{\pm}(J) = T^{\pm} + B^{\pm}J(J+1), \qquad (3.13)$$

are also provided on the plot. Although an insufficient number of J-levels are populated in our experiments to reach the culmination of the perturbation near $J = 9$, the curvature of the measured data points and the fitted curves is evident. The fitted values of $T_{v'}$ and $B_{v'}$ resulting from this deperturbation analysis were not used in the vibrational fit to extract ω_e' and $\omega_e'x_e'$; neither were they used in the rotational fit to extract B_e' and α_e'.

Although the isotope shifts displayed in Fig. 6 show no evidence of perturbations in the $v' = 3$, 4, 5, or 7 levels, the $v' = 3$ level displayed a significantly longer lifetime (2.75 μs) than that found for the $v' = 4$, 5, or 7 levels (which fell within the range of $1.35 \pm 0.22 \mu$s), suggesting that it, too, may be perturbed by another level. The fits of the $v' = 3$, 4, 5, and 7 levels to extract values of ω_e and $\omega_e x_e$ or of B_e and α_e were excellent, however, with largest residuals of 0.5 and 0.0004 cm^{-1}, respectively.

Further similarities to the [22.3]0←X0 system include a large change in bond length upon excitation, leading to band heads at $R(2)$, along with an obvious assignment of the upper state as having $\Omega = 0$, based on the absence of a Q-branch in the rotationally resolved spectra. In addition, like the [22.3]0 state, the [22.1]0 state also has a very low vibrational frequency for a transition metal carbide.

A smattering of other bands appeared in the spectrum. They were all $\Omega' = 0 \leftarrow \Omega'' = 0$ transitions which could not be assigned with certainty as members of a progression, although the bands at 22 053 and 22 569 cm^{-1} have some of the characteristics expected of the unidentified 0–0 and 1–0 bands of the [22.1]0←X0 system: their $\nu_0(^{108}$Pd^{12}C$)$ $- \nu_0(^{105}$Pd^{12}C$)$ isotope shifts are 0.0146 and -0.3926 cm^{-1}; their B' values are 0.4138 and 0.4045 cm^{-1}; and their lifetimes are 1.06 and 2.02 μs, respectively. Extrapolating the fits of the $v' = 3$, 4, 5, and 7 levels of the [22.1]0←X0 system, isotope shifts of 0.256 and -0.418 cm^{-1} and B' values of 0.4012 and 0.3972 cm^{-1} are expected for these bands. It is likely that the upper states of these bands are primarily composed of the $v' = 0$ and 1 levels of the [22.1]0 state, but that homogeneous perturbations among the $\Omega = 0$ states in this energy range have affected these levels so that the bands are shifted considerably from the extrapolated band positions of 22 132 and 22 609 cm^{-1}, respectively.

IV. DISCUSSION

A. Molecular orbitals of PdC and the nature of the ground state

In considering the electronic structure of PdC, it is useful to begin by reviewing the molecular orbitals that may be formed from the atomic orbitals of Pd and C, along with any knowledge that is available for the other $4d$ transition metal carbides. The important molecular orbitals are formed using the $4d_{Pd}$ and $5s_{Pd}$ orbitals of palladium and the $2s_C$ and $2p_C$ orbitals of carbon. As has been discussed in other papers from this group[13-15] and elsewhere, these orbitals combine to give low-lying 10σ, 11σ, and 5π orbitals. The 10σ and 11σ orbitals are somewhat difficult to characterize without detailed calculations, but the 10σ orbital is probably mainly carbon $2s$ in character while the 11σ orbital is probably a

bonding orbital with significant contributions from the $4d\sigma_{Pd}$ and $2p\sigma_C$ orbitals.[39] The 5π orbital is a bonding combination between the $4d\pi_{Pd}$ and $2p\pi_C$ orbitals and is dominated by $4d\pi_{Pd}$ character in an early Hartree–Fock calculation.[39] This was found to be the case in the density functional calculation of Russo *et al.* as well.[41]

Above these bonding orbitals lie the nonbonding 2δ orbitals, which are exclusively palladium $4d\delta$ in character, owing to the lack of accessible δ orbitals on the carbon atom. In RuC and RhC the next orbital above the 2δ orbitals is the 12σ orbital.[39] In these molecules this orbital has been demonstrated to be primarily metal $5s\sigma$ in character, through a comparison of the hyperfine structure of the MC molecule to that of the free metal atom.[12,15] Finally one finds the 6π and 13σ orbitals, which are antibonding in character in the RuC and RhC molecules. In PdC, by contrast, it has been suggested that the 6π orbital is essentially nonbonding and is composed of a nearly pure $2p\pi_C$ atomic orbital, while the 5π orbital retains nearly all of the $4d\pi_{Pd}$ character and is similarly nonbonding in character.[39]

In the ground states of RuC and RhC, the 10σ, 11σ, 5π, and 2δ orbitals are filled, giving ground terms of $10\sigma^2 11\sigma^2 5\pi^4 2\delta^4$, $^1\Sigma^+$ for RuC[15] and $10\sigma^2 11\sigma^2 5\pi^4 2\delta^4 12\sigma^1$, $^2\Sigma^+$ for RhC.[12] It would be reasonable to expect the 12σ orbital to accept one more electron in PdC, to form a $10\sigma^2 11\sigma^2 5\pi^4 2\delta^4 12\sigma^2$, $^1\Sigma^+(\Omega=0^+)$ ground term. However, it is well-known that the $4d$ orbitals drop significantly in energy as one moves across the $4d$ series, particularly relative to the $5s$ orbital.[14] This leads to the unique result that the ground term of atomic Pd is $4d^{10}5s^0$, ^1S, making palladium the only transition metal which lacks valence s electrons in its ground term. The stability of this closed shell configuration contributes to the low bond energies which have been noted for palladium compounds.[39] It is possible that in PdC the ground configuration would avoid placement of two electrons in the $5s$-like 12σ orbital, placing either one or two electrons in the nominally antibonding 6π orbital instead. If only one electron were placed in the 6π orbital, a $10\sigma^2 11\sigma^2 5\pi^4 2\delta^4 12\sigma^1 6\pi^1$, $^3\Pi_r$ ground term would result, for which either the $\Omega=0^+$ or the $\Omega=0^-$ level would be expected to emerge as the ground level. Alternatively, it is conceivable that the 12σ orbital, which is based on the palladium $5s$ atomic orbital, would be so unfavorable that both of the last two electrons would go into the 6π orbital to form a $10\sigma^2 11\sigma^2 5\pi^4 2\delta^4 6\pi^2$, $^3\Sigma^-$ ground term. In the latter case off-diagonal spin–orbit interactions with the higher energy $^1\Sigma^+$ term deriving from the same electronic configuration would cause the ground level to be an $\Omega=0^+$ level. Likewise, if the ground term were $10\sigma^2 11\sigma^2 5\pi^4 2\delta^4 12\sigma^1 6\pi^1$, $^3\Pi_r$, spin orbit interactions between this state and the $10\sigma^2 11\sigma^2 5\pi^4 2\delta^4 12\sigma^2$, $^1\Sigma^+(\Omega=0^+)$ state are calculated to be significant,[42] leading to the emergence of a $^3\Pi_{0+}$ ground spin–orbit level. Thus, regardless of whether the ground term is $^1\Sigma^+$, $^3\Pi_r$, or $^3\Sigma^-$, the ground level is expected to be of $\Omega=0^+$ symmetry.

The R2PI experiments reported here have proven that the ground level of PdC has $\Omega=0$ (and presumably $\Omega=0^+$), but they cannot distinguish between the three competing possibilities of $2\delta^4 12\sigma^2$, $^1\Sigma^+(\Omega=0^+)$;

$2\delta^4 12\sigma^1 6\pi^1$, $^3\Pi_{0+}$; and $2\delta^4 6\pi^2$, $^3\Sigma^-(\Omega=0^+)$ unless additional information is obtained. In dispersed fluorescence experiments to be reported in a subsequent publication, this issue is resolved and the ground state is determined to be the $2\delta^4 12\sigma^2$, $^1\Sigma^+(\Omega=0^+)$ state.[57] All four spin–orbit components of the $2\delta^4 12\sigma^1 6\pi^1$,$^3\Pi$ state are observed in that study, and their $v=0$ levels are found to lie in the range of 2150 to 2850 cm^{-1} above the $v=0$ level of the $2\delta^4 12\sigma^2$, $^1\Sigma^+$ ground state.

The three most recent calculations of PdC are in substantial agreement with our experimental results on the PdC ground state. The density functional calculation of PdC of Russo *et al.* identifies the ground state of PdC as the $2\delta^4 12\sigma^2$, $^1\Sigma^+$ term, with $r_e=1.73$ Å, $\omega_e=907$ cm^{-1}, and $D_e=4.94$ eV.[41] This is in close agreement with our measured value of $r_0=1.712$ Å and with our preliminary value of $\omega_e=844$ cm^{-1} obtained from dispersed fluorescence studies.[57] This level of agreement supports the assignment of the ground state as $2\delta^4 12\sigma^2$, $^1\Sigma^+$, which is analogous to the corresponding $^1\Sigma^+$ ground states of NiC and PtC.[8,9,16] However, this density functional calculation predicts the $2\delta^4 12\sigma^1 6\pi^1$, $^3\Pi$ term to lie only 2718 cm^{-1} above the $^1\Sigma^+$ term, and to have $r_e=1.74$ Å and $\omega_e=794$ cm^{-1}.[41] These two states are calculated to have very similar properties and to lie sufficiently close to one another in energy to prohibit a definite assignment of the ground state based on this calculation alone. The $2\delta^4 6\pi^2$, $^3\Sigma^-$ term, on the other hand, is calculated to have $r_e=1.79$ Å, $\omega_e=642$ cm^{-1}, and to lie 12 164 cm^{-1} above the $^1\Sigma^+$ state. These values differ sufficiently from the values of r_0 and ω_e reported here to allow the $^3\Sigma^-$ term to be discarded as a candidate for the ground state. A particular strength of this density functional study is that the method was tested on the closely related, but experimentally known RhC molecule. There it reproduced the ground state bond length to within 0.03 Å and the vibrational frequency, ω_e, to within 4%. It also reproduced these parameters for the first excited electronic state to within 0.03 Å and 1%, and obtained the energy of the first excited electronic state to within 800 cm^{-1} of the experimental value.

The results of the density functional calculation are borne out to a high degree in the recent CAS–MCSCF–MRSDCI calculation of Tan *et al.*[42] This detailed study obtained a ground term of $2\delta^4 12\sigma^2$, $^1\Sigma^+$, with the $2\delta^4 12\sigma^1 6\pi^1$, $^3\Pi$ term lying 424 cm^{-1} above it when spin–orbit interactions were excluded. The $2\delta^4 12\sigma^2$, $^1\Sigma^+$ ground term had $r_e=1.676$ Å and $\omega_e=822$ cm^{-1}, while the $2\delta^4 12\sigma^1 6\pi^1$, $^3\Pi$ term had $r_e=1.721$ Å and $\omega_e=762$ cm^{-1}. The $2\delta^4 6\pi^2$, $^3\Sigma^-$ term was found to lie 5447 cm^{-1} above the ground state, and had $r_e=1.809$ Å and $\omega_e=664$ cm^{-1}. Based on this study and the previous density functional study of Russo *et al.*,[41] the $2\delta^4 6\pi^2$, $^3\Sigma^-$ term may be eliminated as a candidate for the ground state. However, in both studies the calculated spectroscopic properties of the $2\delta^4 12\sigma^2$, $^1\Sigma^+$ and $2\delta^4 12\sigma^1 6\pi^1$, $^3\Pi$ terms are sufficiently close to those observed here ($r_0=1.712$ Å and $\omega_e=844$ cm^{-1}) that the ground term cannot be assigned on the basis of the level of agreement between experiment and these calculations alone. As mentioned above, dispersed fluorescence studies conducted in this group, to be published else-

where, clearly establish that the ground state is the $2\delta^4\,12\sigma^2$, $^1\Sigma^+$ state.[57]

Finally, a very recent MRCI study by Shim and Gingerich is in good agreement with experiment, predicting the ground state of PdC to be $^1\Sigma^+_{0^+}$ with $\omega_e = 864\,\text{cm}^{-1}$ and $r_e = 1.698\,\text{Å}$.[43]

B. The $[17.9]^3\Sigma^+_1$ state

The $[17.9]^3\Sigma^+_1$ state of PdC is the only state we have observed with Ω different from 0. It therefore is the only state which could possibly display observable hyperfine structure, since all of the states of PdC are expected to be good Hund's case (a) or case (c) states. A simulation of the hyperfine splitting observed in the spectrum of this isotopomer was found to be consistent with that expected from Eq. (3.4), with $|h'| = 0.030 \pm 0.005\,\text{cm}^{-1}$ for the $[17.9]1$ state.

For a system with more than one electron outside of closed shells, Eq. (3.5) must be generalized to[58,59]

$$h = \left\langle \sum_i \left[a_i \hat{l}_{z,i} + \left(b_{Fi} + \frac{2}{3} c_i \right) \hat{s}_{z,i} \right] \right\rangle, \qquad (4.1)$$

where the sum is over all electrons outside of closed shells, with $\hat{l}_{z,i}$ and $\hat{s}_{z,i}$ giving the projections of electronic orbital and spin angular momentum on the axis for electron i. The parameters a_i, b_{Fi}, and c_i are then given by Eqs. (3.6)–(3.8), with the expectation values and $|\psi(0)|^2$ evaluated for electron i. With this in mind, h may be approximated using values of a, b_F, and c based on atomic data. The atomic parameters[60] of $a_{4d}^{01} = -0.006\,02\,\text{cm}^{-1}$, $a_{4d}^{10} = 0.002\,17\,\text{cm}^{-1}$, $a_{5s}^{10} = 0.0598\,\text{cm}^{-1}$, and $a_{4d}^{12} = -0.006\,02\,\text{cm}^{-1}$ correspond to the values of $a_{2\delta}$, $b_{F,2\delta}$, $b_{F,12\sigma}$ and $2/3c_{2\delta}/\langle 3\cos^2\theta - 1\rangle$, assuming that the 2δ and 12σ orbitals are purely $4d\delta_{\text{Pd}}$ and $5s_{\text{Pd}}$ in character, respectively. From these values it is clear that the Fermi contact interaction which results when the $5s$ orbital of palladium is singly occupied is approximately an order-of-magnitude more important than the other sources of hyperfine splitting which arise from the a and c terms. In fact, it is only possible to generate values of h' that are close to the simulated value of $|h'| = 0.030 \pm 0.05\,\text{cm}^{-1}$ for states which place a single, unpaired electron in the 12σ orbital (which is assumed here to be entirely $5s_{\text{Pd}}$ in character). For such a state, the Fermi contact interaction alone contributes $(1/2)0.0598\,\text{cm}^{-1} = 0.0294\,\text{cm}^{-1}$ to the value of $|h'|$, which is nearly sufficient to account for the observed splitting.

The only reasonable electronic configuration for the $[17.9]^3\Sigma^+$ state is a $\sigma^1\sigma^1$ configuration in which one of the unpaired σ electrons has substantial $5s_{\text{Pd}}$ character. The obvious candidate is a $2\delta^4\,12\sigma^1\,13\sigma^1$ configuration. The calculation of Tan et al., predicts the lowest energy $^3\Sigma^+$ state to lie near $14\,477\,\text{cm}^{-1}$, with $\omega_e = 844\,\text{cm}^{-1}$ and $r_e = 1.726\,\text{Å}$ at the MRSDCI level of theory.[42] The state is also calculated to be dominated by the $2\delta^4\,12\sigma^1\,13\sigma^1$ configuration.[42] These values are reasonably close to our measured values of $T_0 = 17\,867\,\text{cm}^{-1}$, $\Delta G_{1/2} = 793.7\,\text{cm}^{-1}$, and $r_e = 1.754\,\text{Å}$. Similar results have been obtained in a very recent calculation by Shim and Gingerich, who find the $^3\Sigma^+$ state at $16\,551\,\text{cm}^{-1}$ with $\omega_c = 902\,\text{cm}^{-1}$ and $r_c = 1.727\,\text{Å}$.[43] Based on the simi-

larity between the calculated and measured properties, it seems fairly certain that the $[17.9]^3\Sigma^+$ state is dominated by the $2\delta^4\,12\sigma^1\,13\sigma^1$ configuration, in agreement with the observed hyperfine structure.

Access to the $2\delta^4\,12\sigma^1\,13\sigma^1$, $^3\Sigma^+_1$ state is spin-forbidden from a ground state that is of pure $2\delta^4\,12\sigma^2$, $^1\Sigma^+$ character, but it may be reached in an allowed one-electron transition from the $2\delta^4\,12\sigma^1\,6\pi^1$, $^3\Pi_{0^+}$ state that is also a candidate for the ground state. If these two states are mixed by spin–orbit interaction, then the $2\delta^4\,12\sigma^1\,13\sigma^1$, $^3\Sigma^+_1$ state may well be spectroscopically accessible even if the ground state is mainly of $2\delta^4\,12\sigma^2$, $^1\Sigma^+$ character. The spin–orbit mixing between the $2\delta^4\,12\sigma^2$, $^1\Sigma^+$ ground state and the $2\delta^4\,12\sigma^1\,6\pi^1$, $^3\Pi_{0^+}$ state will be discussed further in a future publication on the dispersed fluorescence spectra of PdC.[57]

C. The $[22.1]0^+$ and $[22.3]0^+$ states

Only a few $\Omega = 0^+$ candidates for the $[22.1]0^+$ and $[22.3]0^+$ excited states have been calculated thus far.[42] These are the $5\pi^4\,2\delta^3\,12\sigma^1\,6\pi^2$, $^5\Delta$; $5\pi^4\,2\delta^3\,12\sigma^2\,6\pi^1$, $^3\Pi$; and $5\pi^3\,2\delta^4\,12\sigma^1\,6\pi^2$, $^5\Pi$ states, which are calculated at the FOCI level to lie at 18 848, 20 534, and 23 824 cm^{-1}, with $r_e = 1.933$, 1.911, and 2.104 Å and $\omega_e = 540$, 590, and 415 cm^{-1}, respectively. While these states have bond lengths and vibrational frequencies that are similar to those found in our experiments, only the $^3\Pi$ state is accessible from the PdC ground state. Even this state is inaccessible unless the ground $\Omega = 0^+$ state has significant $^3\Pi_{0^+}$ character.

Additional singlet states almost certainly lie in this energy range, and they probably provide the oscillator strength which makes these $\Omega = 0^+$ upper states observable. Likely sources of oscillator strength for these states include the $5\pi^4\,2\delta^4\,12\sigma^1\,13\sigma^1$, $^1\Sigma^+$ and $5\pi^3\,2\delta^4\,12\sigma^2\,6\pi^1$, $^1\Sigma^+$ states.

V. CONCLUSION

Through a laser-ablation, resonant two-photon ionization spectroscopic investigation and comparisons to theoretical calculations, the ground state of ^{108}Pd^{12}C has been determined to be an $\Omega = 0^+$ state with $r_0 = 1.712\,\text{Å}$. Dispersed fluorescence studies, to be reported elsewhere, further establish the ground state to be the $^1\Sigma^+$ state deriving from the $2\delta^4\,12\sigma^2$ configuration.

An excited electronic state lying near $T_0 = 17\,867\,\text{cm}^{-1}$, with $\Omega = 1$, $r_e = 1.754\,\text{Å}$, and $\Delta G_{1/2} = 794\,\text{cm}^{-1}$ is shown to be the $^3\Sigma^+$ state deriving from the $2\delta^4\,12\sigma^1\,13\sigma^1$ configuration. Hyperfine splitting observed in the ^{105}Pd^{12}C isotopic modification demonstrates that either the 12σ or the 13σ orbital consists primarily of palladium $5s$ character. Beyond 21 000 cm^{-1} a number of excited states with $\Omega = 0^+$ have been located, and some of these have been grouped into two band systems. Homogeneous perturbations between these $\Omega = 0^+$ states complicate the interpretation of this portion of the spectrum. Nevertheless, the two $\Omega = 0^+$ states which are identified at $T_0 = 22\,132$ and $22\,251\,\text{cm}^{-1}$ possess r_e values of 1.97 and 1.88 Å, and ω_e values in the neighborhood of 483 and 401 cm^{-1}, respectively. These are

4086   J. Chem. Phys., Vol. 111, No. 9, 1 September 1999   Langenberg, Shao, and Morse

exceptionally long and weak bonds as compared to the known electronic states of other transition metal monocarbides.

ACKNOWLEDGMENTS

[1] W. J. Balfour, J. Cao, C. V. V. Prasad, and C. X. Qian, J. Chem. Phys. **103**, 4046 (1995).

[2] M. D. Allen, T. C. Pesch, and L. M. Ziurys, Astrophys. J. **472**, L57 (1996).

[3] M. Barnes, A. J. Merer, and G. F. Metha, J. Chem. Phys. **103**, 8360 (1995).

[4] A. G. Adam and J. R. D. Peers, J. Mol. Spectrosc. **181**, 24 (1997).

[5] B. Simard, P. A. Hackett, and W. J. Balfour, Chem. Phys. Lett. **230**, 103 (1994).

[6] B. Simard, P. I. Presunka, H. P. Loock, A. Bérces, and O. Launila, J. Chem. Phys. **107**, 307 (1997).

[7] A. J. Marr, M. E. Flores, and T. C. Steimle, J. Chem. Phys. **104**, 8183 (1996).

[8] T. C. Steimle, K. Y. Jung, and B.-Z. Li, J. Chem. Phys. **102**, 5937 (1995).

[9] T. C. Steimle, K. Y. Jung, and B.-Z. Li, J. Chem. Phys. **103**, 1767 (1995).

[10] R. J. Van Zee, J. J. Bianchini, and W. Weltner, Jr., Chem. Phys. Lett. **127**, 314 (1986).

[11] Y. M. Hamrick and W. Weltner, Jr., J. Chem. Phys. **94**, 3371 (1991).

[12] J. M. Brom, Jr., W. R. M. Graham, and W. Weltner, Jr., J. Chem. Phys. **57**, 4116 (1972).

[13] D. J. Brugh and M. D. Morse, J. Chem. Phys. **107**, 9772 (1997).

[14] D. J. Brugh, T. J. Ronningen, and M. D. Morse, J. Chem. Phys. **109**, 7851 (1998).

[15] J. D. Langenberg, R. S. DaBell, L. Shao, D. Dreessen, and M. D. Morse, J. Chem. Phys. **109**, 7863 (1998).

[16] D. J. Brugh and M. D. Morse (unpublished).

[17] R. Scullman and B. Thelin, Phys. Scr. **3**, 19 (1971).

[18] R. Scullman and B. Thelin, Phys. Scr. **5**, 201 (1972).

[19] A. Lagerqvist, H. Neuhaus, and R. Scullman, Z. Naturforsch. A **20a**, 751 (1965).

[20] A. Lagerqvist and R. Scullman, Ark. Fys. **32**, 475 (1966).

[21] B. Kaving and R. Scullman, J. Mol. Spectrosc. **32**, 475 (1969).

[22] H. Neuhaus, R. Scullman, and B. Yttermo, Z. Naturforsch. A **20a**, 162 (1965).

[23] R. Scullman and B. Yttermo, Ark. Fys. **33**, 231 (1966).

[24] O. Appelblad, R. F. Barrow, and R. Scullman, Proc. Phys. Soc. London **91**, 260 (1967).

[25] O. Appelblad, C. Nilsson, and R. Scullman, Phys. Scr. **7**, 65 (1973).

[26] K. Jansson, R. Scullman, and B. Yttermo, Chem. Phys. Lett. **4**, 188 (1969).

[27] K. Jansson and R. Scullman, J. Mol. Spectrosc. **36**, 248 (1970).

[28] C. W. Bauschlicher, Jr. and P. E. M. Siegbahn, Chem. Phys. Lett. **104**, 331 (1984).

[29] I. Shim and K. A. Gingerich, Int. J. Quantum Chem. **42**, 349 (1992).

[30] I. Shim, M. Pelino, and K. A. Gingerich, J. Chem. Phys. **97**, 9240 (1992).

[31] I. Shim, H. C. Finkbiner, and K. A. Gingerich, J. Phys. Chem. **91**, 3171 (1987).

[32] M. D. Hack, R. G. A. R. Maclagan, G. E. Scuseria, and M. S. Gordon, J. Chem. Phys. **104**, 6628 (1996).

[33] R. G. A. R. Maclagan and G. E. Scuseria, Chem. Phys. Lett. **262**, 87 (1996).

[34] R. G. A. R. Maclagan and G. E. Scuseria, J. Chem. Phys. **106**, 1491 (1997).

[35] H. Tan, M. Liao, and K. Balasubramanian, Chem. Phys. Lett. **280**, 423 (1997).

[36] H. Tan, M. Liao, and K. Balasubramanian, Chem. Phys. Lett. **280**, 219 (1997).

[37] D. Majumdar and K. Balasubramanian, Chem. Phys. Lett. **284**, 273 (1998).

[38] I. Shim and K. A. Gingerich, J. Chem. Phys. **76**, 3833 (1982).

[39] I. Shim and K. A. Gingerich, Surf. Sci. **156**, 623 (1985).

[40] G. Pacchioni, J. Koutecký, and P. Fantucci, Chem. Phys. Lett. **92**, 486 (1982).

[41] N. Russo, J. Andzelm, and D. R. Salahub, Chem. Phys. **114**, 331 (1987).

[42] H. Tan, D. Dai, and K. Balasubramanian, Chem. Phys. Lett. **286**, 375 (1998).

[43] I. Shim and K. A. Gingerich (personal communication).

[44] S. C. O'Brien, Y. Liu, Q. Zhang, J. R. Heath, F. K. Tittel, R. F. Curl, and R. E. Smalley, J. Chem. Phys. **84**, 4074 (1986).

[45] P. R. Bevington, *Data Reduction and Error Analysis for the Physical Sciences* (McGraw-Hill, New York, 1969).

[46] S. Gerstenkorn and P. Luc, *Atlas du Spectre d'Absorption de la Molecule d'Iode entre 14,800–20,000 cm^{-1}* (CNRS, Paris, 1978).

[47] S. Gerstenkorn and P. Luc, Rev. Phys. Appl. **14**, 791 (1979).

[48] S. Gerstenkorn, J. Verges, and J. Chevillard, *Atlas du Spectre d'Absorption de la Molecule d'Iode entre 11,000–14,000 cm^{-1}* (CNRS, Paris, 1982).

[49] J. Cariou and P. Luc, *Atlas du Spectre d'Absorption de la Molécule Tellure, Partie 5: 21,100–23,800 cm^{-1}* (CNRS, Paris, 1980).

[50] J. M. Brown and A. J. Merer, J. Mol. Spectrosc. **74**, 488 (1979).

[51] H. Lefebvre-Brion and R. W. Field, *Perturbations in the Spectra of Diatomic Molecules*, 1st ed. (Academic, Orlando, 1986).

[52] J. T. Hougen, *The Calculation of Rotational Energy Levels and Rotational Line Intensities in Diatomic Molecules* (US GPO, Washington, D.C., 1970).

[53] See, AIP Document No. PAPS JCPSA6-111-005931 for 30 pages of absolute line positions, fits of B_v values, and vibronic fits. Order by PAPS number and journal reference from American Institute of Physics, Physics Auxiliary Publication Service, Suite 1NO1, 2 Huntington Quadrangle, Melville, NY 11747-4502. Fax: 516-576-2223, e-mail: paps@aip.org. The price is $1.50 for each microfiche (98 pages) or $5.00 for photocopies up to 30 pages, and $0.15 for each additional page over 30 pages. Airmail additional. Make checks payable to the American Institute of Physics.

[54] R. A. Frosch and H. M. Foley, Phys. Rev. **88**, 1337 (1952).

[55] W. Weltner, Jr., *Magnetic Atoms and Molecules* (Dover Publications, Inc., New York, 1983).

[56] G. Herzberg, *Molecular Spectra and Molecular Structure I. Spectra of Diatomic Molecules*, 2nd ed. (Van Nostrand Reinhold, New York, 1950).

[57] R. DaBell, R. Meyer, and M. D. Morse (unpublished).

[58] T. M. Dunn, in *Molecular Spectroscopy: Modern Research*, edited by K. N. Rao and C. W. Mathews (Academic, New York and London, 1972), pp. 231.

[59] C. H. Townes and A. L. Schawlow, *Microwave Spectroscopy* (Dover Publications, Inc., New York, 1975).

[60] S. Büttgenbach, *Hyperfine Structure in 4d- and 5d-Shell Atoms* (Springer, Berlin, Heidelberg, New York, 1982).